New conjunctive CubeSat and balloon measurements to quantify rapid energetic electron precipitation

L. W. Blum,[1,2] Q. Schiller,[1,2] X. Li,[1,2] R. Millan,[3] A. Halford,[3] and L. Woodger[3]

Received 31 October 2013; accepted 2 November 2013; published 22 November 2013.

[1] Relativistic electron precipitation into the atmosphere can contribute significant losses to the outer radiation belt. In particular, rapid narrow precipitation features termed precipitation bands have been hypothesized to be an integral contributor to relativistic electron precipitation loss, but quantification of their net effect is still needed. Here we investigate precipitation bands as measured at low earth orbit by the Colorado Student Space Weather Experiment (CSSWE) CubeSat. Two precipitation bands of MeV electrons were observed on 18–19 January 2013, concurrent with precipitation seen by the 2013 Balloon Array for Radiation belt Relativistic Electron Losses (BARREL) campaign. The newly available conjugate measurements allow for a detailed estimate of the temporal and spatial features of precipitation bands for the first time. We estimate the net electron loss due to the precipitation bands and find that ~20 such events could empty the entire outer belt. This study suggests that precipitation bands play a critical role in radiation belt losses. **Citation:** Blum, L. W., Q. Schiller, X. Li, R. Millan, A. Halford, and L. Woodger (2013), New conjunctive CubeSat and balloon measurements to quantify rapid energetic electron precipitation, *Geophys. Res. Lett.*, *40*, 5833–5837, doi:10.1002/2013GL058546.

1. Introduction

[2] The outer radiation belt is a highly dynamic region of Earth's magnetosphere, with often unpredictable variations in intensity and spatial extent. The physical processes controlling the acceleration and loss of trapped relativistic electrons in the radiation belts are complex, and there are a number of competing processes that produce net enhancements or depletions of the belts. Particle precipitation into the atmosphere is a critical part of radiation belt electron loss; without quantified understanding of this loss mechanism, we are unable to fully understand acceleration mechanisms. In particular, rapid electron precipitation is often observed at low altitude on a variety of timescales ranging from short bursts of less than 1 s (microbursts) to longer duration precipitation extending a few degrees in latitude (termed precipitation bands, following *Blake et al*. [1996]). These precipitation bands have been hypothesized to be an integral contributor to storm time relativistic electron precipitation loss [*Bortnik et al*., 2006], but quantification of their net contribution is still needed.

[3] Precipitation bands, also referred to as "spikes" historically [e.g., *Brown and Stone*, 1972], have been observed by a number of satellites in low earth orbit (LEO). They occur both during quiet and more active times, primarily across the afternoon and night sectors [*Imhof et al*., 1986; *Nakamura et al*., 2000]. Their 5–30 s duration, as observed by LEO satellites, is thought to be spatial rather than temporal, as precipitation bands are often seen on consecutive orbits and in conjugate hemispheres [*Nakamura et al*., 1995]. Their exact temporal duration is difficult to estimate from a single LEO satellite alone.

[4] Wave-particle interaction theory predicts rapid precipitation events to occur on the duskside due to pitch angle scattering of MeV electrons by electromagnetic ion cyclotron (EMIC) waves [*Thorne and Kennel*, 1971]. *Vampola* [1971] suggested that a subset of the precipitation bands measured by the OV3-3 satellite at LEO were the observational signatures of EMIC wave-MeV electron interactions. *Imhof et al*. [1986] found a correspondence between the radial location of precipitation bands and the plasmapause, as well as concurrent keV ion precipitation on a few occasions, further supporting EMIC waves as a cause of the bands. Electrostatic waves and pitch angle scattering at the trapping boundary have also been proposed precipitation band generation mechanisms [*Koons et al*., 1972; *Brown and Stone*, 1972]. Data from the Solar Anomalous and Magnetospheric Particle Explorer (SAMPEX)/Heavy Ion Large Telescope (HILT) instrument, which measures a combination of trapped and precipitating > 1 MeV electrons and provides some pitch angle distribution information, suggest fluxes become isotropic during these band features, indicating a rapid scattering mechanism and precipitation of the electrons into the atmosphere [*Blake et al*., 1996; *Li et al*., 1997].

[5] Historically, electron precipitation has also been investigated by balloon campaigns measuring bremsstrahlung X-rays produced by precipitating electrons as they collide with neutrals in the atmosphere (see *Parks et al*. [1993] for a review). *Foat et al*. [1998] presented the first reported measurement of X-rays extending up to MeV energies, indicating relativistic electron precipitation or "REP". Using measurements from the MeV Auroral X-ray Imaging and Spectroscopy (MAXIS) balloon payload, *Millan et al*. [2002] found that REP events were constrained to the afternoon sector, between noon and midnight, while softer precipitation was measured across the full range of local times. SAMPEX/HILT measurements also indicate that harder precipitation events preferentially occur in the afternoon, night and dawn sectors, with a peak occurrence around 22 magnetic local time (MLT) at an L shell of 5–6 [*Comess et al*., 2013]. However, due to the inherently

[1]Department of Aerospace Engineering Sciences, University of Colorado Boulder, Boulder, Colorado, USA.
[2]Laboratory for Atmospheric and Space Physics, Boulder, Colorado, USA.
[3]Department of Physics and Astronomy, Dartmouth College, Hanover, New Hampshire, USA.

Corresponding author: L. W. Blum, Department of Aerospace Engineering Sciences, University of Colorado Boulder, Boulder, CO 80303, USA. (lauren.blum@colorado.edu)

0094-8276/13/10.1002/2013GL058546

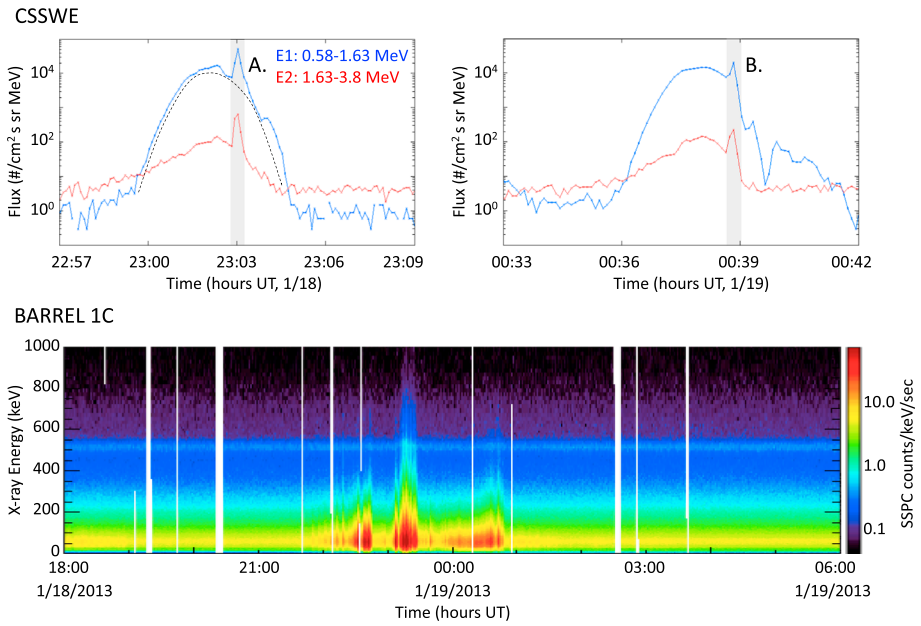

Figure 1. (top) Measurements from the CSSWE CubeSat and (bottom) BARREL balloon 1C during a precipitation event on 18–19 January 2013. CSSWE measures two precipitation bands (labeled A and B and indicated by the shaded grey regions) on two consecutive passes through the outer belt. The dashed black line suggests the background trapped and bounce loss cone flux upon which the precipitation bands are superimposed. (bottom) X-ray spectra from balloon 1C are shown from 18:00 UT 18 January through 06:00 UT 19 January. During this time, three main precipitation events are measured by the balloon, the second two showing X-rays of energies >0.5 MeV. No background subtraction has been applied here to either the BARREL or CSSWE measurements.

different nature of the observations, the exact relationship between the precipitation bands observed at LEO and the REP events seen by balloons is still uncertain.

[6] Here we investigate precipitation bands, as measured at LEO by the Colorado Student Space Weather Experiment (CSSWE) CubeSat [*Li et al*., 2012, 2013a]. Two precipitation bands were observed by CSSWE on 18–19 January 2013, concurrent with relativistic electron precipitation seen by the Balloon Array for Radiation belt Relativistic Electron Losses (BARREL) [*Millan et al*., 2013]. These magnetically conjugate observations confirm the link between precipitation bands and balloon-measured REP and can be used to constrain the duration and extent of the precipitation bands. We calculate the net electron loss due to these precipitation bands and compare to the total radiation belt content at the time. The newly available differential flux measurements from CSSWE, combined with the spatial coverage of the array of BARREL balloons, allow a detailed quantification of precipitation band loss for the first time.

2. Observations

2.1. Instrument Descriptions

[7] The CSSWE CubeSat, designed, built, and operated by students at the University of Colorado, was launched from Vandenberg Airforce Base on 13 September 2012 into a 65° inclination, 480 × 780 km altitude orbit [*Li et al*., 2013a]. The sole science payload onboard is the Relativistic Electron and Proton Telescope integrated little experiment (REPTile), a miniaturized version of the Relativistic Electron and Proton Telescope (REPT) instrument [*Baker et al*., 2012] onboard NASA/Van Allen Probes [*Kessel et al*., 2012]. This instrument provides 6 s directional, differential electron flux in three energy ranges: 0.58–1.63, 1.63–3.8, and > 3.8 MeV. With a field of view of 52° pointing within 15° of perpendicular to the background magnetic field, REPTile measures a combination of trapped and precipitating particles, similar to the SAMPEX/HILT instrument. Details on the instrument design and calibration can be found in *Schiller and Mahendrakumar* [2010] and *Blum and Schiller* [2012], and the data processing and conversion to flux are described in *Li et al*. [2013b]. Care has been taken to remove noise due to temperature variations and radio transmissions.

[8] Data from the 2013 BARREL campaign are also examined here. Roughly five balloons, distributed in local time and magnetic latitude, were taking measurements at 27–37 km over Antarctica on any given day throughout the January–February 2013 campaign. These balloons carry X-ray spectrometers sensitive to bremsstrahlung X-rays ranging from 20 keV up to 10 MeV. Using Monte Carlo simulations and a forward-folding technique, described in detail in *Millan et al*. [2013], one can estimate the energy spectrum of the incident precipitating electrons from the measured X-ray spectrum [e.g., *Foat et al*., 1998; *Millan et al*., 2007]. Here, however, we use the X-ray measurements simply as an indication of energetic electron precipitation and the CSSWE measurements to determine exact electron energies and fluxes.

2.2. The 18–19 January 2013 Precipitation

[9] On 18-19 January 2013, CSSWE observed two large precipitation bands of MeV electrons. Concurrently, payload 1C of BARREL measured X-rays due to energetic electron precipitation. Figure 1 (top) shows the electron flux during two passes of CSSWE through the outer radiation belt on consecutive orbits. Superimposed atop the smoothly varying background of trapped and drift loss cone electrons (as

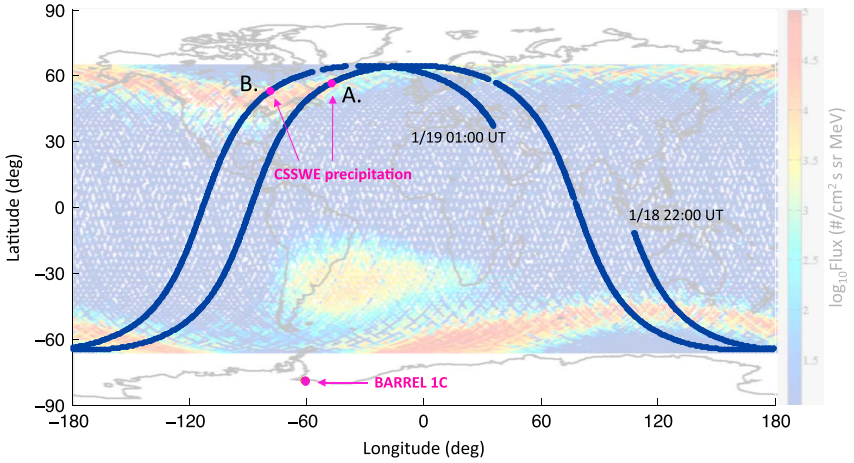

Figure 2. The ground track of CSSWE from 22:00 UT 18 January through 01:00 UT 19 January is shown in dark blue, with the location of precipitation bands A and B in pink (band labels are consistent throughout all figures). BARREL balloon 1C was located in the Southern Hemisphere at a conjugate location during this period. The 0.58–1.63 MeV electron measurements from CSSWE during a 2 week period are plotted on the color scale in the background to show typical inner and outer belt sampling by the CubeSat from its low-altitude orbit.

indicated by the dashed black curve), a distinct rapid flux enhancement is seen at 23:03 UT 18 January and again around 00:39 UT 19 January. Figure 1 (bottom) shows the X-ray spectrum measured by BARREL balloon 1C during this same time period. Three large precipitation events are seen, the second two extending to energies > 0.5 MeV. Figure 2 shows the location of the two precipitation bands along the ground track of the CubeSat, as well as the balloon 1C position from 22:00 UT 18 January to 01:00 UT 19 January. The background color indicates 0.58—1.63 MeV electron flux measurements from CSSWE over a 2 week period, to demonstrate the typical sampling of the outer and inner radiation belts from the CubeSat orbit. CSSWE is in the Northern Hemisphere during both the precipitation band observations, while BARREL is in the Southern, supporting the idea that the bands are an indication of rapid pitch angle scattering causing simultaneous electron precipitation in both hemispheres.

[10] To better investigate the location and timing of the precipitation observed by CSSWE and balloon 1C, their positions are mapped to the magnetic equatorial plane using the T89 magnetic field model [*Tsyganenko*, 1989], with real-time *Kp* as input (*Kp* varies between 2 and 3+ during this period). The T89 model has been shown to perform well on the duskside during quiet to moderate geomagnetic conditions such as these [*McCollough et al.*, 2008]. Figure 3 shows the CubeSat and balloon locations in this plane in L shell and magnetic local time (MLT). The color bar here indicates universal time of their positions. The periods of precipitation have been marked with black circles; these include the two precipitation bands measured by CSSWE and the second two precipitation periods measured by BARREL around 23:15 UT 18 January and 00:35 UT 19 January. The first precipitation band measured by CSSWE at 23:03 UT 18 January lines up with the third precipitation region seen by BARREL balloon 1C almost 2 h later. The second band, measured by CSSWE at 00:39 UT 19 January, is aligned with the precipitation measured by balloon 1C ~23:15 UT 18 January. From this figure, it is evident that the precipitation bands agree in both L and MLT with precipitation seen by BARREL. These magnetically conjugate observations suggest that at least some precipitation bands measured at LEO are the same phenomenon as the REP events seen by balloons.

3. Discussion: Loss Calculation

[11] The balloon and LEO satellite measurements combine to constrain the temporal and spatial features of the

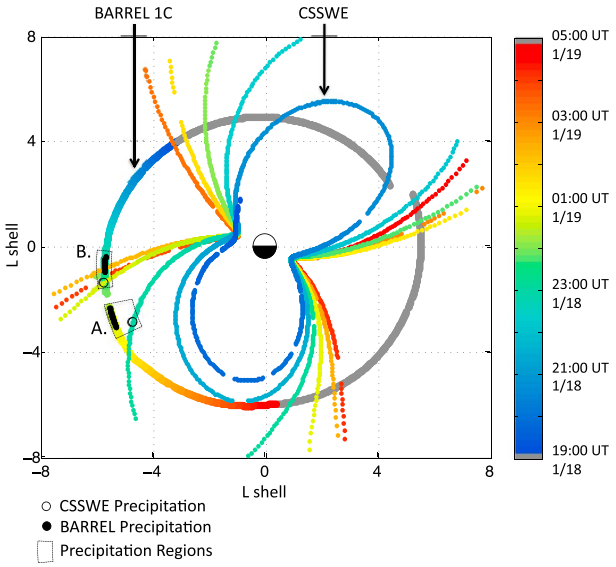

Figure 3. The location of CSSWE and balloon 1C mapped to the magnetic equatorial plane, with local noon at the top. Universal time of the locations is shown on the color bar. The balloon drifts across the dusk sector at a fairly constant L ~ 5.5–6, while the CubeSat cuts across this track every roughly 90 min. The locations of the precipitation bands, as measured by CSSWE, are indicated by the open black circles. The tracks of solid black circles indicate when balloon 1C measures >0.5 MeV X-rays due to precipitating electrons. The dotted boxes outline the two precipitation regions as determined from the conjunctive measurements, (exact dimensions of these regions are listed in Table 1).

Table 1. The Parameters Used to Calculate Area and Total Loss for Precipitation Bands A and B (as Labeled in Figures 1–3)

	Band A			Band B		
Universal Time (UT)	Start: 23:03 1/18[a]	Stop: 00:50 1/19	Δ: 01:47 h	Start: 23:05 1/18	Stop: 00:39 1/19	Δ: 1:34 h
Magnetic Local Time (MLT)	Start: 19:30	Stop: 20:00	Δ: 0.5 h	Start: 18:12	Stop: 18:42	Δ: 0.5 h
Magnetic Latitude (MLAT)	Start: 66.95°	Stop: 65.15°	Δ: 1.8°	Start: 63.1°	Stop: 62.6°	Δ: 0.5°
0.58–1.6 MeV Flux	Peak: 5.3×10^4	Background: 7.7×10^3	Δ: 4.5×10^4	Peak: 2.0×10^4	Background: 6.0×10^3	Δ: 1.4×10^4
1.6–3.8 MeV Flux	Peak: 661.1	Background: 64.42	Δ: 596.68	Peak: 218.5	Background: 34.74	Δ: 183.76

[a]Dates are formatted as month/day.

precipitation bands. The balloons measure the azimuthal extent of the precipitation in local time, while the bands measured by CSSWE indicate a narrow radial width of the precipitation regions, consistent with a lack of precipitation observed by additional balloons at L ~ 4 and L ~ 8 also in the dusk sector. Combined, they bound the physical dimensions of the precipitation regions, as well as place constraints on the duration of the event in UT. The dashed black boxes in Figure 3 outline the precipitation regions estimated from the balloon and CubeSat measurements, with exact dimensions listed in Table 1. While the end time of the events is fairly well constrained by subsequent CubeSat passes through the region, these measurements provide only a lower bound on the UT duration, as the precipitation may have begun before the CubeSat and balloons moved into this duskside region.

[12] Using these estimates of the dimensions and duration of the precipitation bands, we are thus able to calculate a lower limit to the overall loss of energetic electrons into the atmosphere during this event. Following the technique used by *Lorentzen et al*. [2001] and *O'Brien et al*. [2004] to estimate losses measured by SAMPEX, we calculate the electron flux through the area of the precipitation regions at the altitude of CSSWE using the following equation:

$$\#e- = 2\cdot\Delta f\cdot\Delta T\cdot A\cdot 2\pi$$

where Δf is the magnitude of the precipitation band above the background trapped and drift loss cone flux (e.g., solid minus dashed line in Figure 1 (top), ΔT the duration of the precipitation in UT, and A the area of the precipitation region at the CubeSat altitude. The factor 2 comes from assuming conjugate precipitation in both hemispheres and 2π from an assumption of isotropy over the down-going hemisphere.

[13] Table 1 lists these parameters estimated for precipitation bands A and B, as determined from Figures 1–3. For band A, we calculate an area of 8.35×10^{14} cm^2 and a loss of 2.5×10^{24} electrons in CSSWE's first energy channel and 6.6×10^{22} in the second channel. Band B gives an area of 2.6×10^{14} cm^2 and a loss of 2.2×10^{23} electrons in the first energy channel and 5.8×10^{21} in the second. Combined, these bands produce a total loss of ~2.7×10^{24} 0.58–1.63 MeV electrons and 7.2×10^{22} 1.63–3.8 MeV electrons. For this analysis, we have chosen to group the precipitation measurements by physical location (MLT) rather than UT and magnitude. However, if instead we group precipitation measurements by UT (band A measured by CSSWE paired with precipitation seen by BARREL ~23:15 UT on 18 January) and interpret the events as two shorter duration (~30 min) precipitation regions spanning the duskside from 17:30–20:00 MLT, we get a total loss within a factor of 1.5 of the above calculation. While the observations cannot necessarily distinguish between these two scenarios (two longer duration but narrower in local time precipitation regions versus larger but shorter duration regions), the exact interpretation of the precipitation structure does not significantly affect the results.

[14] For comparison, *Millan et al*. [2002] estimated that a precipitation event measured by the MAXIS balloon in January 2000 produced a loss of ~ 5×10^{25} >0.5 MeV electrons over the course of 8 days. Another type of rapid precipitation, microbursts, was found by *O'Brien et al*. [2004] to contribute ~10^{23} >1 MeV electrons during one pass of SAMPEX through the outer belt, while *Lorentzen et al*. [2001] calculate a loss of ~10^{24} for the same pass using a less sophisticated calculation method.

[15] To put these numbers into context, a quick estimate of the total radiation belt content can be made following *O'Brien et al*. [2004]. Using CSSWE measurements of the trapped outer belt population and assuming a $\sin^n$ form of the pitch angle distribution with n = 2.5 [*Gannon et al*., 2007], we integrate flux over pitch angle and L shell volume from L = 3–6.5. This produces a total electron content of ~7×10^{25} for 0.58–1.63 MeV electrons and 2×10^{24} for 1.63–3.8 MeV electrons. If we look at just the drift shells right around the precipitation region (~L = 5.5–5.8), we estimate the content to be ~1/10th that of the whole belt.

[16] As shown by these calculations, the precipitation events on 18–19 January 2013 produced a significant amount of loss, precipitating roughly half the content of their given drift shell and at least 5% of the total outer radiation belt content at the time. Events such as these could easily empty entire drift shells in a few hours, and approximately 20 of them could empty the outer radiation belt. While geomagnetic conditions were relatively mild during this event (Dst ~ −20 nT following a moderate storm on 17 January) and precipitation band occurrence rates are expected to be low during quiet times, ~1–10% [*Nakamura et al*., 2000], occurrences have been observed to increase during more active periods. During a large storm on 20 November 2003, over 60 precipitation bands were measured by SAMPEX over the 3 day storm [*Bortnik et al*., 2006]. During that storm, as well as others, precipitation bands potentially contributed a large amount of radiation belt electron loss. Whether these losses lead to radiation belt dropouts and depletions depends upon competing acceleration mechanisms and will be the focus of future work. This study indicates that precipitation losses must be taken into account when studying outer radiation belt dynamics and that precipitation bands, more specifically, can contribute significant rapid losses that may not be fully accounted for if looking only at longer time-averaged precipitation rates.

4. Conclusions

[17] This study combines differential energy measurements of rapid energetic electron precipitation observed by the CSSWE CubeSat at LEO with precipitation measured at lower altitude by BARREL. Magnetically conjugate measurements

of simultaneous precipitation observed by the CubeSat and balloon 1C on 18-19 January 2013 help constrain the dimensions and duration of the precipitation regions. The combination of these new measurements enables a detailed estimate of MeV electron loss due to precipitation bands for the first time, to our knowledge. We find that the loss of 0.58–1.63 and 1.63–3.8 MeV electrons during this event was at least 5% of the total outer radiation belt content. The following points summarize the findings of this study:

[18] 1. Conjunctive measurements confirm the association between "precipitation band" measurements made by satellites at LEO [e.g., *Brown and Stone*, 1972; *Vampola*, 1971; *Imhof et al*., 1986; *Blake et al*., 1996] and relativistic electron precipitation "REP" measured by balloons at lower altitude [e.g., *Foat et al*., 1998; *Millan et al*., 2002].

[19] 2. New measurements from CubeSat and balloon payloads are combined here to estimate the spatial and temporal characteristics of two duskside precipitation events.

[20] 3. Quantification of the MeV electron loss due to the measured precipitation bands indicates that ~20 such events could empty the entire outer radiation belt.

[21] Using newly available measurements from the CSSWE and BARREL missions in support of the Van Allen Probes, this study demonstrates that precipitation bands, commonly observed during geomagnetic storms, play an important role in outer radiation belt dynamics and losses.

[22] **Acknowledgments.** This work was supported in part by the CSSWE funding grant NSF AGSW 0940277 as well as the NASA Earth and Space Sciences Fellowship (NESSF) award NNX12AL75H. The Dartmouth College portion of this work was supported by NASA grant NNX08AM58G. We would also like to acknowledge the BARREL and CSSWE teams for their efforts and in particular, Hong Zhao, Brett Anderson, and Sam Califf for their contributions and helpful discussion.

[23] The Editor thanks two anonymous reviewers for their assistance in evaluating this paper.

References

Baker, D. N., et al. (2012), The Relativistic Electron-Proton Telescope (REPT) instrument on board the Radiation Belt Storm Probes (RBSP) spacecraft: Characterization of Earth's radiation belt high-energy particle populations, *Space Sci. Rev.*, *179*, 337–381, doi:10.1007/s11214-012-9950-9.

Blake, J. B., M. D. Looper, D. N. Baker, R. Nakamura, B. Klecker, and D. Hovestadt (1996), New high temporal and spatial resolution measurements by SAMPEX of the precipitation of relativistic electrons, *Adv. Space Res.*, *18*(8), 171–186.

Blum, L. W. and Q. G. Schiller (2012), Characterization and testing of an energetic particle telescope for a CubeSat platform, Small Satellite Conference, AIAA/USU.

Bortnik, J., R. M. Thorne, T. P. O'Brien, J. C. Green, R. J. Strangeway, Y. Y. Shprits, and D. N. Baker (2006), Observation of two distinct, rapid loss mechanisms during the 20 November 2003 radiation belt dropout event, *J. Geophys. Res.*, *111*, A12216, doi:10.1029/2006JA011802.

Brown, J. W., and E. C. Stone (1972), High-energy electron spikes at high latitudes, *J. Geophys. Res.*, *77*, 3384–3396.

Comess, M. D., D. M. Smith, R. S. Selesnick, R. M. Millan, and J. G. Sample (2013), Duskside relativistic electron precipitation as measured by SAMPEX: A statistical survey, *J. Geophys. Res. Space Physics*, *118*, 5050–5058, doi:10.1002/jgra.50481.

Foat, J. E., R. P. Lin, D. M. Smith, F. Fenrich, R. Millan, I. Roth, K. R. Lorentzen, M. P. McCarthy, G. K. Parks, and J. P. Treilhou (1998), First detection of a terrestrial MeV X-ray burst, *Geophys. Res. Lett.*, *25*, 4109–4112.

Gannon, J. L., X. Li, and D. Heynderickx (2007), Pitch angle distribution analysis of radiation belt electrons based on Combined Release and Radiation Effects Satellite Medium Electrons A data, *J. Geophys. Res.*, *112*, A05212, doi:10.1029/2005JA011565.

Imhof, W. L., H. D. Voss, D. W. Datlowe, E. E. Gaines, J. Mobilia, and D. S. Evans (1986), Relativistic electron and energetic ion precipitation spikes near the plasmapause, *J. Geophys. Res.*, *91*, 3077–3088.

Kessel, R. L., N. J. Fox, and M. Weiss (2012), The Radiation Belt Storm Probes (RBSP) and space weather, *Space Sci. Rev.*, *179*, 531–543, doi:10.1007/s11214-012-9953-6.

Koons, H. C., A. L. Vampola, and D. A. McPherson (1972), Strong pitch-angle scattering of energetic electrons in the presence of electrostatic waves above the ionospheric trough region, *J. Geophys. Res.*, *77*(10), 1771–1775.

Li, X., D. Baker, M. Temerin, T. E. Cayton, E. G. D. Reeves, R. A. Christensen, J. B. Blake, M. D. Looper, R. Nakamura, and S. G. Kanekal (1997), Multisatellite observations of the outer zone electron variation during the November 3-4, 1993, magnetic storm, *J. Geophys. Res.*, *102*, 14,123–14,140.

Li, X., et al. (2012), Colorado Student Space Weather Experiment: Differential flux measurements of energetic particles in a highly inclined low Earth orbit, in *Dynamics of the Earth's Radiation Belts and Inner Magnetosphere*, Geophys. Monogr. Ser., vol. 199, edited by D. Summers et al., pp. 385-404, AGU, Washington, D. C., doi:10.1029/2012GM001313.

Li, X., S. Palo, R. Kohnert, L. Blum, D. Gerhardt, Q. Schiller, and S. Califf (2013a), Small mission accomplished by students—Big impact on Space Weather Research, *Space Weather*, *11*, 55–56, doi:10.1002/swe.20025.

Li, X., et al. (2013b), First results from CSSWE: Characteristics of relativistic electrons in the near-earth environment during the October 2012 magnetic storms, *J. Geophys. Res. Space Physics*, *118*, 1–11, doi:10.1002/2013JA019342.

Lorentzen, K. R., M. D. Looper, and J. B. Blake (2001), Relativistic electron microbursts during the GEM storms, *Geophys. Res. Lett.*, *28*, 2573–2576.

McCollough, J. P., J. L. Gannon, D. N. Baker, and M. Gehmeyr (2008), A statistical comparison of commonly used external magnetic field models, *Space Weather*, *6*, S10001, doi:10.1029/2008SW000391.

Millan, R. M., R. P. Lin, D. M. Smith, K. R. Lorentzen, and M. P. McCarthy (2002), X-ray observations of MeV electron precipitation with a balloon-borne germanium spectrometer, *Geophys. Res. Lett.*, *29*(24), 2194, doi:10.1029/2002GL015922.

Millan, R. M., R. P. Lin, D. M. Smith, and M. P. McCarthy (2007), Observation of relativistic electron flux, *Geophys. Res. Lett*, *34*, L10101, doi:10.1029/2006GL028653.

Millan, R. M., et al. (2013), The Balloon Array for RBSP Relativistic Electron Losses (BARREL), *Space Sci. Rev.*, *179*, 503–530, doi:10.1007/s11214-013-9971-z.

Nakamura, R., D. N. Baker, J. B. Blake, S. Kanekal, B. Klecker, and D. Hovestadt (1995), Relativistic electron precipitation enhancements near the outer edge of the radiation belt, *J. Geophys. Res.*, *22*, 1129–1132.

Nakamura, R., M. Isowa, Y. Kamide, D. N. Baker, J. B. Blake, and M. Looper (2000), SAMPEX observations of precipitation bursts in the outer radiation belt, *J. Geophys. Res.*, *105*, 15,875–15,886.

O'Brien, T. P., M. D. Looper, and J. B. Blake (2004), Quantification of relativistic electron microburst losses during the GEM storms, *Geophys. Res. Lett*, *31*, L04802, doi:10.1029/2003GL018621.

Parks, G. K., T. J. Freeman, M. P. McCarthy, and S. H. Werden (1993), The discovery of auroral X-rays by balloon-borne detectors and their contributions to magnetospheric research, in *Auroral Plasma Dynamics*, Geophys. Monogr. Ser., vol. 80, edited by R. L. Lysak, pp. 17–23, AGU, Washington, D. C., doi:10.1029/GM080p0017.

Schiller, Q. and A. Mahendrakumar (2010), REPTile: A miniaturized detector for a CubeSat mission to measure relativistic particles in near-earth space, Small Satellite Conference, AIAA/USU.

Thorne, R. M., and C. F. Kennel (1971), Relativistic electron precipitation during magnetic storm main phase, *J. Geophys. Res.*, *76*, 4446–4453.

Tsyganenko, N. A. (1989), A magnetospheric magnetic field model with a warped tail current sheet, *Planet. Space Sci.*, *37*, 5–20, doi:10.1016/0032-0633(89)90066-4.

Vampola, A. L. (1971), Electron pitch angle scattering in the outer zone during magnetically disturbed times, *J. Geophys. Res.*, *76*, 4685.